Chapter 8

Iodide-Mediated Gaseous Ozone Oxidation of Aerosol Bromide and Chloride as a Possible Source of Gaseous Marine Halogens

Sections reprinted with permission from Enami, S.; Vecitis, C. D.; Cheng, J.; Hoffmann, M. R.; Colussi, A. J. *Journal of Physical Chemistry A* **2007**, *111*, 8749-8752.

Abstract

A few gaseous bromine molecules per trillion (ppt) cause the complete destruction of ozone in the lower troposphere during the polar sunrise and about half of the losses associated with the ‘ozone hole’ in the stratosphere. Recent field measurements of BrO in the free troposphere suggest an even more global role of atmospheric bromine. Models quantifying ozone trends by assuming atmospheric inorganic bromine (Br_y) stems exclusively from long-lived bromoalkane gases significantly underpredict BrO measurements. This discrepancy implies a tropospheric background level of ~ 4 ppt Br_y of unknown origin. Here we report that I^- efficiently mediates the oxidation of Br^- and Cl^- in aqueous droplets exposed to gaseous ozone. Br^- and Cl^-, which are kinetically unreactive towards O_3 in comparison to I^-, and were previously deemed unlikely direct precursors of atmospheric halogens, are readily converted into IBr_2^- and ICl_2^- in the presence of I^- and gaseous ozone. Fine sea salt aerosol particles ($r < 1$ micron) are reported to be enriched in I^- and Br^- and may be a global source of photoactive gaseous halogen compounds in the atmosphere even in the absence of sunlight.

Introduction

Bromine critically affects atmospheric ozone at all altitudes, playing a crucial role in the ozone depletion events (ODEs) observed in the polar lower troposphere during early spring[1-3]. Despite its lower abundance, bromine is 45–70 times more efficient than chlorine as a catalyst of stratospheric ozone depletion[4]. The mechanism of atmospheric bromine production from its primary seawater bromide source is not fully understood[5]. It has been generally assumed that gaseous inorganic bromine (Br_y) is released in the stratosphere by the short wavelength photolysis of long-lived source gases, such as biogenic methyl bromide and anthropogenic halons[6]. However, recent field (surface station, balloon, and satellite) BrO measurements, which are broadly consistent with each other, significantly exceed model predictions based on those BrO source assumptions[7–9] The implication is that some Br_y is directly delivered to the free troposphere, possibly carried by sea salt aerosol itself[8,10–12]. Marine aerosols appear to be plausible vehicles for halogen activation since a fraction of the sea spray aerosols are fine ($r < 1$ micron) particles that remain suspended long enough to undergo chemical processing.

Polar ODEs require the presence of appreciable levels ($\gtrsim$10 ppt) of rapidly photolyzable $Br_2(g)$ in the boundary layer at the end of the polar winter night[13-15]. Since ODEs are also observed under pristine Antarctic conditions, the conversion of marine Br^- into $Br_2(g)$ should involve an oxidant that persists in the dark, such as O_3. The inertness of Br^- and Cl^- towards O_3 is circumvented in sea salt as compared to NaCl and NaBr alone[16]. That significantly more $Br_2(g)$ is emitted from sea salt than from pure NaBr exposed to $O_3(g)$ implies that Br^- oxidation is catalyzed or mediated by a minor component of the sea salt[17]. I^- is one viable sea salt component since it reacts at diffusion-controlled rates with ozone. Halogen activation may also occur to some extent on the surface of sea ice, which has been reported to catalyze a number of atmospherically relevant reactions.

The enrichment of seawater anions such as Br^- and I^- in fine marine aerosol particles would be expected to enhance the possible halogen activation[18–20]. Relative anion populations, f_i, at the interface of droplets produced from equimolar solutions were recently shown to increase exponentially with ionic radius r_i, i.e.: $f_i \propto \exp(\beta\, r_i)$, $f_{I^-}/f_{Br^-} = 5.2$, $f_{Br^-}/f_{Cl^-} = 3.4$.[21] This correlation reveals that anion fractionation at the air/water interface is simply another manifestation of the Hofmeister effects generally observed at aqueous interfaces in contact with less polarizable media.[22] The enrichment of Br^- and I^- in fine aerosol particles of greater surface-area-to-volume ratios would be expected to enhance oxidation kinetics by ozone, which partitions weakly to the aqueous phase from the gas phase, via reactions at the air-water interface.

We investigated this possibility in laboratory experiments where the reaction products of aqueous halide droplets sprayed into an $O_3(g)$ plume are monitored via online electrospray mass spectrometry (ESMS) of the evaporated anions (Figure 6.1).

Small drops are usually charged, even when produced by fragmentation of electrically neutral liquids, due to statistical fluctuations that scale with (drop size)$^{-1/2}$ [23]. For example, submicron marine aerosol drops are, on average, negatively charged[24]. Water evaporation regulated by ambient relative humidity will eventually shrink the suspended droplets, subsequently increasing electrostatic repulsion among excess surface charges. Coulomb explosions may ensue if charge density is great enough and highly charged droplets lose interfacial charge and mass into smaller droplets[25]. These events, if replicated by the subsequent droplets, generate small particles that are enriched (i.e., net enrichment $\propto (f_i)^m$, where m is the number of successive Coulomb explosions) in Br^- and I^-. This mechanism provides a physicochemical (i.e., abiotic)[1,26] explanation for anion enrichment in aerosol particles, as well as for its inverse dependence on particle size and statistical variations among individual particles of similar size[19]. Anion enrichment may also be partially due to droplet acidification resulting in protonation and then gasification of the weaker acids. Smaller particles drawing mass and surface charge from larger units is consistent with observations that Br^- is enriched in submicron particles while depleted in larger specimens[2].

Figure 8.1a shows the extent of I^- oxidation in aqueous NaI microdroplets injected in $O_3(g)$ gas mixtures at atmospheric pressure. Interfacial I^- concentration decreases by ~ 50% after exposure to $[O_3(g)] \simeq 100$ ppm for $\simeq 1$ to 10 ms (i.e., I^- reacts with O_3 with an apparent pseudo-first-order rate constant, $k^I \sim 10^3\ s^{-1}$, that can be formally calculated from the reaction rate constant in bulk solution: $k^{II}(I^- + O_3)_{aq} = 1.2 \times 10^9\ M^{-1}\ s^{-1}$ [28], and $[O_3(aq)] \sim 1\ \mu M$ (from Henry's law constant $H = 0.01\ M\ atm^{-1}$ for O_3 in water at 298 K). I^- oxidation proceeds at rates R_{-I^-} given by: $R_{-I^-} \propto [I^-]^n\ [O_3(g)]$. The actual n value may be obtained from the fact that at steady state: $IF(I^-) - [I^-]\ \tau^{-1} - k_R\ [I^-]^n\ [O_3(g)] = 0$, where $IF(I^-)$ is the I^- inflow to the reaction zone, i.e., the intersection between the droplets and the $O_3(g)$ plumes in Figure 6.1, τ is the transit time through this zone, k_R the overall reaction rate constant, and n the effective kinetic order of $[I^-]$ in eq. 8.1[29]. Since: $IF(I^-) - [I^-]_0\ \tau^{-1} = 0$ at $[O_3(g)] = 0$, a plot of $([I^-]_0 - [I^-])/[I^-]^n$ vs. $[O_3(g)]$ should be linear. The data of Figure 8.1a are linearized provided that $\langle n \rangle = 0.67 \pm 0.03$ in the range $1 \le [NaI]/\mu M \le 30$ ($[I^-] = 0.5\ \mu M$ in seawater) (Figure 8.1b). In this context $0.5 \le \langle n \rangle \le 1$ is an empirical parameter that encodes the competition between mass transfer and chemical reaction at the gas-liquid interface. We actually verified that $\langle n \rangle \rightarrow 1$ as $[I^-] \rightarrow 500$ μM, as expected for a surface-specific gas-liquid reaction[30,31]. From these experiments, we estimate that it takes ~ 40 minutes to oxidize 50% of the iodide contained in microdroplets suspended in typical ~ 40 ppb (parts per billion) atmospheric $O_3(g)$ concentrations. R_{-I^-} is independent of bulk pH in the range 4.0 to 7.0. However, this calculation assumes that ozone is only reacting with I^- in the aerosols, which is a poor assumption given that a similar or greater concentration of more surface-active organics that will also react at diffusion-controlled rates with ozone will be found in the marine aerosols.

The simultaneous detection of iodate, IO_3^- (m/z = 175), and triiodide, I_3^- (m/z = 381), as products of I^- oxidation by O_3 in this system implies that their putative precursor, the HOI intermediate formed in eq. 8.1

$$I^- + O_3 + H^+ = HOI + O_2 \tag{8.1}$$

also has a reactive half-life shorter than ~ 1 to 10 ms. This finding is, however, at odds with estimates based on bulk solution kinetic data and conditions. From $k^{II}(HOI + O_3)_{aq} = 3.6 \times 10^4\ M^{-1}\ s^{-1}$ [32], $k^{II}(HOI + I^- + H^+)_{aq} = 4.4 \times 10^{12}\ M^{-2}\ s^{-1}$ [33], $[O_3(aq)] \sim 1$ μM, $[I^-] \sim 10$ μM, at pH ~ 7 we estimate HOI half-lives toward oxidation by O_3 ($t_{1/2} = 19$ s) and reaction with I^- ($t_{1/2} = 0.16$ s) that are significantly longer than 1 ms. As expected from Scheme 8.1, the $[IO_3^-]/[I_3^-]$ ratio is an increasing function of $[O_3(g)]$ (Figure 8.2). Relative interfacial anion concentrations were derived from ESMS signal intensities S corrected by the response factors: $[IO_3^-]/[I^-] = 0.80 \times S(IO_3^-)/S(I^-)$, and $[I_3^-]/[I^-] = 0.76 \times S(I_3^-)/S(I^-)$, determined under present experimental conditions. Note that the detected I_3^-, which is presumably involved in the fast equilibrium: $I_2 + I^- \leftrightarrow I_3^-$ ($K_{eq} = 740\ M^{-1}$), must actually desorb from microdroplets in which [I^-] necessarily exceeds the μM range. Thus, while I^- is oxidized to HOI immediately after the droplets enter the $O_3(g)$ plume, subsequent chemistry takes place in the increasingly concentrated aqueous media resulting from rapid solvent evaporation due to high (10 L/min) and hot (250° C) dry N_2 cross-flows [25]. Similar conditions are expected to develop, albeit at a slower pace, in the marine aerosol as they rise into the dry atmosphere[34]. IO_3^- and I_3^- yields calculated from interfacial I^- losses (m/z = 127) circumstantially exceed unity, revealing that interfacial layers are competitively replenished with I^- from the droplets core. These results suggest that the rates and mechanisms of chemical reactions at aerosol interfaces cannot be directly inferred from those in bulk solution[35].

We confirmed that aqueous Br^- and Cl^- are inert toward O_3 under present conditions, in line with reported rate constants $k^{II}(Br^- + O_3)_{aq} = 248\ M^{-1}\ s^{-1}$ [28], and $k^{II}(Cl^- + O_3)_{aq} = 0.1\ M^{-1}\ s^{-1}$, that are $\gtrsim 10^7$ times smaller than $k^{II}(I^- + O_3)_{aq}$ in bulk solution. However, ozonation experiments performed on (NaI + NaBr) and (NaI + NaCl) solutions readily yield the trihalide anions IBr_2^- and ICl_2^- (Figures 8.3a and 8.3b). IBr_2^- and ICl_2^- production rates increase with [$O_3(g)$] (Figure 8.4) while Br^- inhibits I^- depletion and depresses IO_3^- and I_3^- formation (Figure 8.5). IBr_2^- and ICl_2^- are, therefore, the products of Br^- and Cl^- oxidation by I-containing intermediates, such as HOI or the primary adduct I-OOO$^-$, that are considerably more reactive than O_3. Since rate constants for the reactions of halide anions with HOI are similar ($I^- \sim Br^- \sim 10\ Cl^-$)[36] the huge selectivity of the stronger oxidizer O_3 for I^- vs. Br^-/Cl^- is counterintuitive. Note that spin conservation requires the formation of excited $O_2(^1\Delta_g)$ in eq. 8.1. This restriction is more likely to be lifted by I^- than by Br^- or Cl^- via heavy atom enhancement of crossing rates into the triplet manifold that leads to ground state $O_2(^3\Sigma_g)$[37]. By mitigating spin conservation constraints, eq. 8.1 becomes the gateway to the I^--mediated production of Br_2 (and Cl_2) from sea salt (Scheme 8.1). The efficiency of this cycle (i.e., the $[Br_2]/[IO_3^-]$ ratio) is expected to be a direct function of $[Br^-]/[O_3]$ at the droplets interface. Since Cl^- will always be present in large excess ($[Cl^-]/[Br^-]/[I^-] = 1.1 \times 10^6/1680/1$ in seawater) sea salt particles exposed to O_3(g) will generate IBr_2^- and ICl_2^- rather than I_3^-, depending on actual interfacial halide and $[O_3(g)]$, and some Br^- will remain even after extensive atmospheric processing. Scheme 8.1 actually provides a plausible mechanism for buffering the $[IO_3^-]/[I^-]$ ratio[38].

Present experiments and analysis suggest that I^- may be the ‘minor component’ that enhances O_3 uptake and concomitant Br_2 formation in sea salt.[17] The iodide-mediated oxidation cycle in Scheme 8.1 qualifies as the previously unidentified dark process that may liberate dihalogens such as IBr(g), ICl(g), or even Cl_2(g) and Br_2(g) from sea salt into the boundary layer during the polar winter night[15]. The accumulation of these species on aerosol surfaces or in the atmosphere would prime the sudden destruction of O_3 at polar sunrise due to their quick photolysis ($\tau_{1/2} \sim 1$ to 2 min)[1]. The proposed mechanism of marine halide ozone oxidation should operate over the oceans worldwide, rather than just around coastal regions, at rates that may be locally modulated by wind speed, relative humidity, and atmospheric ozone concentration[8]. The fast halogen activation rates demonstrated by our experiments may exceed aerosol transport rates. In summary, fine marine aerosols are expected to be naturally enriched in I^- and Br^-, and the oxidation of these species by reactive gases such as ozone may release gaseous halogen species into the atmosphere even in the absence of sunlight. Further experiments will be completed to evaluate this process under more environmental conditions.

Figures

Figure 8.1. Normalized iodide concentrations $[I^-]/[I^-]_0$ vs. $[O_3(g)]$ A) (▼): 1 μM. (●): 10 μM. (▲) : 30 μM NaI) droplets. B) Linearized plot of the data of Figure 8.1a. See text. (▼): 1 μM; (●): 10 μM; (▲) : 30 μM NaI

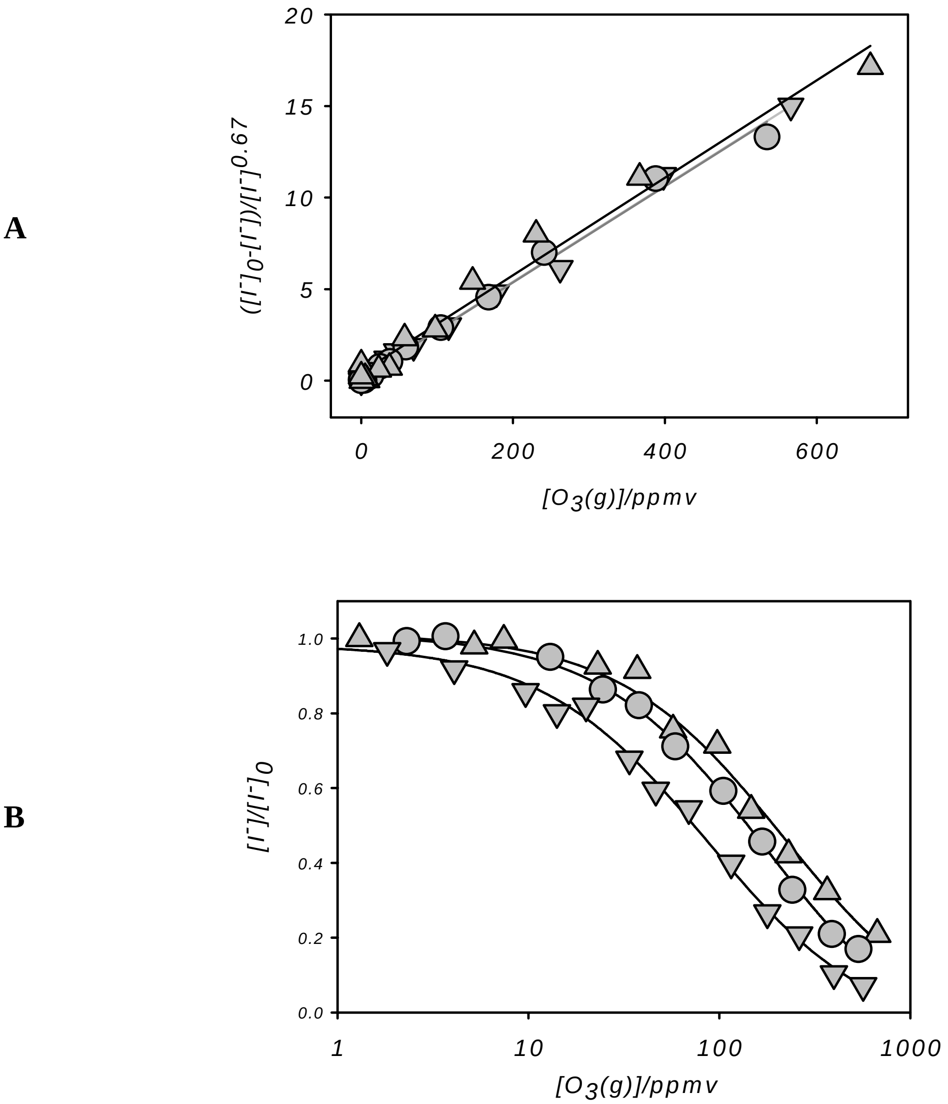

Figure 8.2. $[IO_3^-]/[I_3^-]$ ratio as function of $[O_3(g)]$. (▼): 1 µM; (●): 10 µM; (▲) :30 µM NaI. The straight line corresponds to a linear $[IO_3^-]/[I_3^-]$ vs. $[O_3(g)]$ dependence

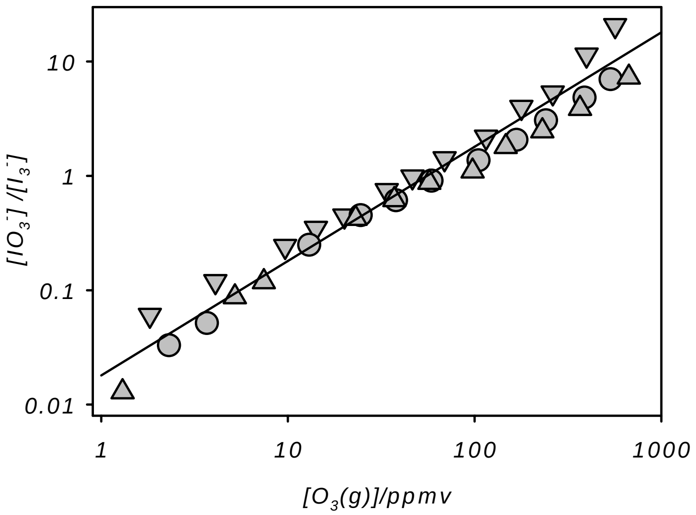

Figure 8.3. Aqueous NaBr-NaI or NaCl-NaI and $O_{3(g)}$ reaction products. A) Negative ion mass spectra of aqueous (10 µM NaI + 100 µM NaBr) droplets. **Blue trace**: Mass spectrum in 1 atm N_2. Peak 1: m/z = 127 (I^-). Peak group 2: m/z = 181, 183, and 185 ($NaBr_2^-$). **Red trace**: Mass spectrum in [840 ppm O_3(g) + 1 atm N_2] gas mixtures. Peak X: m/z = 175 (IO_3^-). Peak group Y: m/z = 285 ($I^{79}Br^{79}Br^-$), m/z = 287 ($I^{79}Br^{81}Br^-$), m/z = 289 ($I^{81}Br^{81}Br^-$). Peak Z: m/z = 381 (I_3^-). B) Negative ion mass spectra of aqueous (10 µM NaI + 10 mM NaCl) droplets. **Blue trace**: mass spectrum in 1 atm N_2. Peak 1: m/z = 127 (I^-). Peak group 2: m/z = 151, 153, 155, and 157 ($Na_2Cl_3^-$). Peak group 3: m/z = 209 to 217 ($Na_3Cl_4^-$). **Red trace**: mass spectrum in [690 ppm O_3(g) + 1 atm N_2] gas mixtures. Peak X: m/z = 175 (IO_3^-). Peak group W: m/z = 197 ($I^{35}Cl^{35}Cl^-$), m/z = 199 ($I^{35}Cl^{37}Cl^-$), m/z = 201 ($I^{37}Cl^{37}Cl^-$)

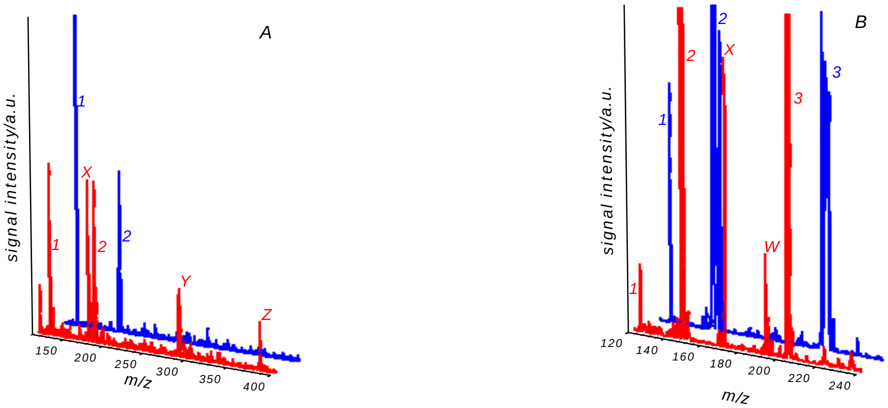

Figure 8.4. Aqueous NaBr-NaI or NaCl-NaI and $O_{3(g)}$ reaction products vs. $[O_{3(g)}]$. (▲): m/z = 287 ($I^{79}Br^{81}Br^-$) from ([NaI] = 10 μM + [NaBr] = 5 mM) droplets. (▼): m/z = 197 ($I^{35}Cl^{35}Cl^-$) from (10 μM NaI + 10 mM NaCl) droplets

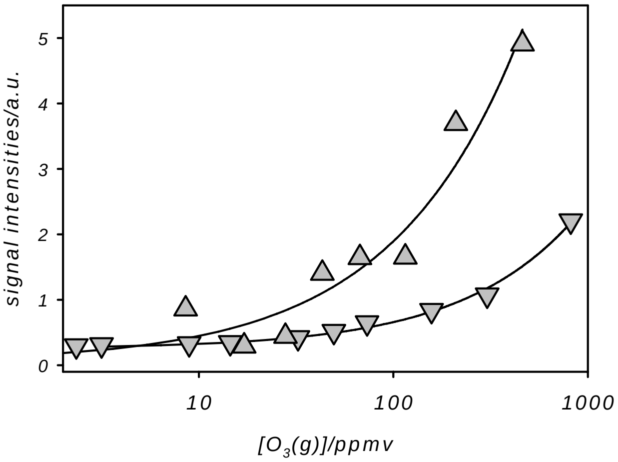

Figure 8.5. Aqueous NaBr-NaI and NaI and $O_{3(g)}$ reaction products vs. $[O_{3(g)}]$. (○): experiments in 10 μM NaI. (●): experiments in (10 μM NaI + 1 mM NaBr). ○: m/z = 127 (I^-); △: m/z = 175 (IO_3^-); ▽: m/z = 381 (I_3^-)

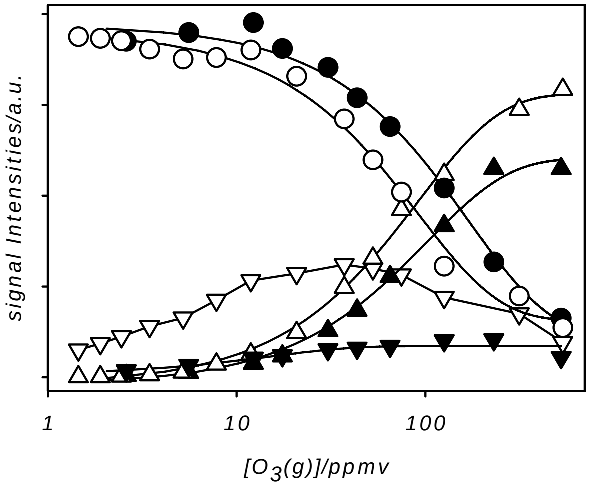

Scheme 8.1. Representation of iodide-mediated ozone oxidation of chloride and bromide

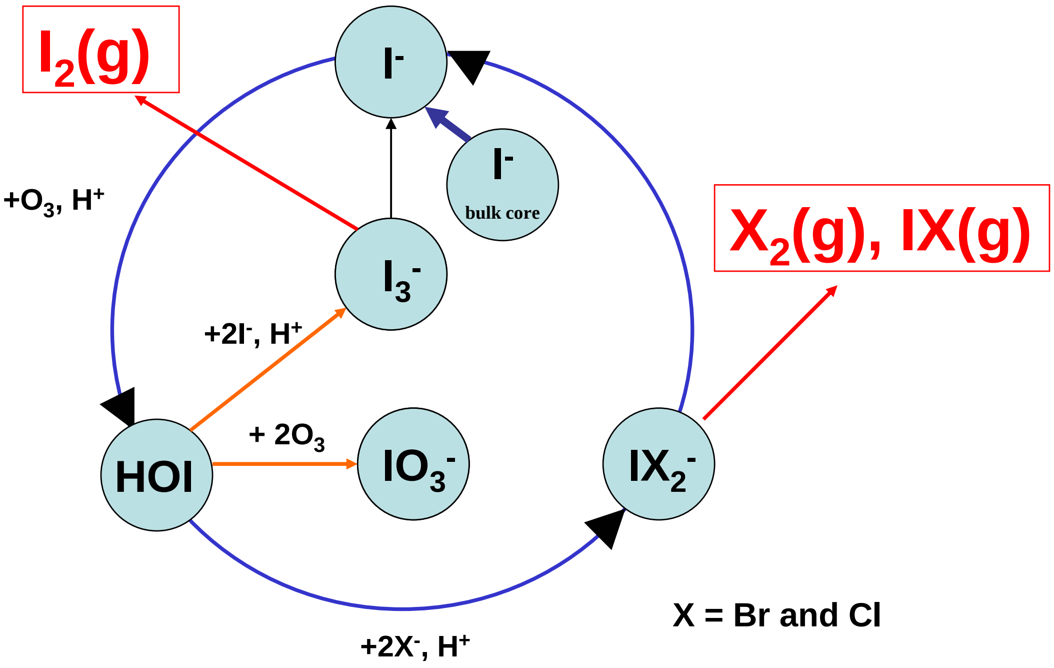

References

(1) Barrie, L. A.; Bottenheim, J. W.; Schnell, R. C.; Crutzen, P. J.; Rasmussen, R. A. *Nature* **1988**, *334*, 138.

(2) Sander, R.; Keene, W. C.; Pszenny, A. A. P.; Arimoto, R.; Ayers, G. P.; Baboukas, E.; Cainey, J. M.; Crutzen, P. J.; Duce, R. A.; Honninger, G.; Huebert, B. J.; Maenhaut, W.; Mihalopoulos, N.; Turekian, V. C.; Van Dingenen, R. *Atmos. Chem. Phys.* **2003**, 1301.

(3) Yang, X.; Cox, R. A.; Warwick, N. J.; Pyle, J. A.; Carver, G. D.; O'Connor, F. M.; Savage, N. H. *J. Geophys. Res.* **2005**, *110*, D23311.

(4) Sinnhuber, B. M.; Sheode, N.; Sinnhuber, M.; Chipperfield, M. P. *Atmos. Chem. Phys. Discuss.* **2006**, 6497.

(5) Simpson, W. R.; Von Glasow, R.; Riedel, K.; Anderson, P.; Ariya, P.; Bottenheim, J. W.; Burrows, J.; Carpenter, L.; Friess, U.; Goodsite, M. E.; Heard, D.; Hutterli, M.; Jacobi, H. W.; Kaleschke, L.; Neff, B.; Plane, J.; Platt, U.; Richter, A.; Roscoe, H.; Sander, R.; Shepson, P. B.; Sodeau, J.; Steffen, A.; Wagner, T.; Wolff, E. *Atmos. Chem. Phys. Discuss.* **2007**, *7*, 4285.

(6) World Metereological Organization (WMO), *Global Ozone Research and Monitoring Project*, *Scientific Assessment of Ozone Depletion: 2002, Report No. 47*; Geneva, 2003.

(7) Sioris, C. E.; Kovalenko, L. J.; McLinden, C. A.; Salawitch, R. J.; Van Roozendael, M.; Goutail, F.; Dorf, M.; Pfeilsticker, K.; Chance, K.; von Savigny, C.; Liu, X.; Kurosu, T. P.; Pommereau, J. P.; Bosch, H.; Frerick, J. *J. Geophys. Res.* **2006**, *111*, D14301.

(8) Dorf, M.; Butler, J. H.; Butz, A.; Camy-Peyret, C.; Chipperfield, M. P.; Kritten, L.; Montzka, S. A.; Simmes, B.; Weidner, F.; Pfeilsticker, K. *Geophys. Res. Lett.* **2006**, *33*, L24803.

(9) Schofield, R.; Johnston, P. V.; Thomas, A.; Kreher, K.; Connor, B. J.; Wood, S.; Shooter, D.; Chipperfield, M. P.; Richter, A.; von Glasow, R.; Rodgers, D. C. *J. Geophys. Res.* **2006**, *111*, D22310.

(10) Salawitch, R. J. *Nature* **2006**, *439*, 275.

(11) Salawitch, R. J.; Weisenstein, D. K.; Kovalenko, L. J.; Sioris, C. E.; Wennberg, P. O.; Chance, K.; Ko, M. K. W.; McLinden, C. A. *Geophys. Res. Lett.* **2005**, *32*, L05811.

(12) von Glasow, R.; von Kuhlmann, R.; Lawrence, M. G.; Platt, U.; Crutzen, P. J. *Atmos. Chem. Phys.* **2004**, *4*, 2481.

(13) Li, S. M.; Yokouchi, Y.; Barrie, L. A.; Muthuramu, K.; Shepson, P. B.; Bottenheim, J. W.; Sturges, W. T.; Landsberger, S. *J. Geophys. Res.* **1994**, *99*, 25415.

(14) Foster, K. L.; Plastridge, R. A.; Bottenheim, J. W.; Shepson, P. B.; Finlayson-Pitts, B. J.; Spicer, C. W. *Science* **2001**, *291*, 471.

(15) Hara, K.; Osada, K.; Matsunaga, K.; Iwasaka, Y.; Shibata, T.; Furuya, K. *J. Geophys. Res.* **2002**, *107*, D4361.

(16) Finlayson-Pitts, B. J. *Chem. Rev.* **2003**, *103*, 4801.

(17) Mochida, M.; Hirokawa, J.; Akimoto, H. *Geophys. Res. Lett.* **2000**, *27*, 2629.

(18) Lewis, E. R.; Schwartz, S. E. *Sea Salt Aerosol Production: Mechanisms, Methods, Measurements and Models—A Critical Review*, Vol. Geophysical Monograph 152; American Geophysical Union: Washington, D.C., **2004**.

(19) Murphy, D. M.; Thomson, D. S.; Middlebrook, A. M. *Geophys. Res. Lett.* **1997**, *24*, 3197.

(20) Murphy, D. M.; Cziczo, D. J.; Froyd, K. D.; Hudson, P. K.; Matthew, B. M.; Middlebrook, A. M.; Peltier, R. E.; Sullivan, A.; Thompson, D. S.; Weber, R. J. *J. Geophys. Res.* **2006**, *111*, D23S32.

(21) Cheng, J.; Vecitis, C.; Hoffmann, M. R.; Colussi, A. J. *J. Phys. Chem. B* **2006**, *110*, 25598.

(22) Pegram, L. M.; Record, M. T. *J. Phys. Chem. B* **2007**, *111*, 5411.

(23) Dodd, E. E. *J. Appl. Phys.* **1953**, *24*, 73.

(24) Reiter, R. *J. Geophys. Res.* **1994**, *99*, 10807.

(25) Kebarle, P. *J. Mass Spectrom.* **2000**, *35*, 804.

(26) Carpenter, L. J.; Hopkins, J. R.; Jones, C. E.; Lewis, A. C.; Parthipan, R.; Wevill, D. J. *Environ. Sci. Technol.* **2005**, *39*, 8812.

(27) Simpson, W. R.; Alvarez-Aviles, L.; Douglas, T. A.; Sturm, M.; Domine, F. *Geophys. Res. Lett.* **2005**, *32*, L04811.

(28) Liu, Q.; Schurter, L. M.; Muller, C. E.; Aloisio, S.; Francisco, J. S.; Margerum, D. W. *Inorg. Chem.* **2001**, *40*, 4436.

(29) Colussi, A. J.; Baghal-Vayjooee, M. H.; Benson, S. W. *J. Am. Chem. Soc.* **1978**, *100*, 3214.

(30) Davidovits, P.; Kolb, C. E.; Williams, L. R.; Jayne, J. T.; Worsnop, D. R. *Chem. Rev.* **2006**, *106*, 1323.

(31) Hanson, D. R. *J. Phys. Chem. B* **1997**, *101*, 4998.

(32) Bichsel, Y.; von Gunten, U. *Environ. Sci. Technol.* **1999**, *33*, 4040.

(33) Eigen, M.; Kustin, K. *J. Am. Chem. Soc.* **1962**, *84*, 1355.

(34) Gao, Y.; Chen, S. B.; Yu, L. E. *Atmos. Environ.* **2007**, *41*, 2019.

(35) Hunt, S. W.; Roeselova, M.; Wang, W.; Wingen, L. M.; Knipping, E. M.; Tobias, D. J.; Dabdub, D.; Finlayson-Pitts, B. J. *J. Phys. Chem. A* **2004**, *108*, 11559.

(36) Vogt, R.; Sander, R.; von Glasow, R.; Crutzen, P. J. *J. Atmos. Chem.* **1999**, *32*, 375.

(37) Muñoz, F.; Mvula, E.; Braslavsky, S. E.; von Sonntag, C. *J. Chem. Soc. Perkin Trans. 2* **2001**, 1109.

(38) Bruchert, W.; Helfrich, A.; Zinn, N.; Klimach, T.; Breckenheimer, M.; Chen, H.; Lai, S.; Hoffmann, T.; Bettmer, J. *Anal. Chem.* **2007**, *79*, 1714.